



SOX2 Reprograms Resident Astrocytes into Neural Progenitors in the Adult Brain

Wenze Niu,^{1,2} Tong Zang,^{1,2} Derek K. Smith,^{1,2} Tou Yia Vue,³ Yuhua Zou,^{1,2} Robert Bachoo,⁴ Jane E. Johnson,³ and Chun-Li Zhang^{1,2,*}

¹Department of Molecular Biology

²Hamon Center for Regenerative Science and Medicine

³Department of Neuroscience

⁴Department of Neurology and Neurotherapeutics

University of Texas Southwestern Medical Center, 6000 Harry Hines Boulevard, Dallas, TX 75390, USA

*Correspondence: chun-li.zhang@utsouthwestern.edu

<http://dx.doi.org/10.1016/j.stemcr.2015.03.006>

This is an open access article under the CC BY-NC-ND license (<http://creativecommons.org/licenses/by-nc-nd/4.0/>).

SUMMARY

Glial cells can be *in vivo* reprogrammed into functional neurons in the adult CNS; however, the process by which this reprogramming occurs is unclear. Here, we show that a distinct cellular sequence is involved in SOX2-driven *in situ* conversion of adult astrocytes to neurons. This includes ASCL1⁺ neural progenitors and DCX⁺ adult neuroblasts (iANBs) as intermediates. Importantly, ASCL1 is required, but not sufficient, for the robust generation of iANBs in the adult striatum. These progenitor-derived iANBs predominantly give rise to calretinin⁺ interneurons when supplied with neurotrophic factors or the small-molecule valproic acid. Patch-clamp recordings from the induced neurons reveal subtype heterogeneity, though all are functionally mature, fire repetitive action potentials, and receive synaptic inputs. Together, these results show that SOX2-mediated *in vivo* reprogramming of astrocytes to neurons passes through proliferative intermediate progenitors, which may be exploited for regenerative medicine.

INTRODUCTION

Neurons in the CNS are particularly sensitive to injury and degenerative conditions that frequently result in cell death. Although adult neurogenesis persists in restricted brain areas (Gage, 2000; Hsieh, 2012; Kriegstein and Alvarez-Buylla, 2009; Lie et al., 2004), neurons do not regenerate in most regions of the adult CNS. An unmet challenge in neural injury and degeneration repair is how to replenish lost neurons for functional recovery.

Cell fate reprogramming provides new means for regenerating damaged or dead neurons (Arlotta and Berninger, 2014; Cherry and Daley, 2012; Matsui et al., 2014). Not only can cells in culture be reprogrammed into pluripotent stem cells (Takahashi and Yamanaka, 2006), lineage-restricted stem cells (Kim et al., 2011a; Ring et al., 2012), and different postmitotic cell fates (Heinrich et al., 2010, 2011; Karow et al., 2012; Liu et al., 2013; Vierbuchen et al., 2010), but they are also amenable to *in vivo* fate conversion (Guo et al., 2014; Heinrich et al., 2014; Niu et al., 2013; Qian et al., 2012; Song et al., 2012; Su et al., 2014a, b; Torper et al., 2013; Zhou et al., 2008). In regards to the CNS, resident glial cells have been directly or indirectly converted into functional neurons in the adult brain and spinal cord (Guo et al., 2014; Heinrich et al., 2014; Niu et al., 2013; Su et al., 2014a, b; Torper et al., 2013). Glial cells are broadly distributed and comprise nearly half of the cells in the mammalian CNS. These cells become reactive, proliferate, and form glial scars in response to neural injuries and degen-

eration (Karimi-Abdolrezaee and Billakanti, 2012; Sofroniew, 2009). These reactive responses are initially beneficial, restricting the spread of damage, but ultimately are deleterious, acting as both a physical and chemical barrier to neuronal regeneration (Karimi-Abdolrezaee and Billakanti, 2012; Sofroniew, 2009). Reprogramming some of these glial cells to functional neurons may constitute a novel therapeutic strategy for diseases associated with the CNS.

Through *in vivo* screens of candidate factors that are able to induce neurogenesis in non-neurogenic regions of the adult brain and spinal cord, we previously showed that the ectopic expression of SOX2 is sufficient to reprogram resident astrocytes to DCX⁺ induced adult neuroblasts (iANBs) (Niu et al., 2013; Su et al., 2014a). These iANBs pass through a proliferative state and generate mature neurons when supplied with neurotrophic factors. This SOX2-driven *in vivo* reprogramming process sharply contrasts direct lineage conversion strategies (Guo et al., 2014; Qian et al., 2012; Song et al., 2012; Su et al., 2014b; Torper et al., 2013; Zhou et al., 2008), which change cell fate in a linear fashion without amplification of the induced cell population. However, the cellular mechanism underlying SOX2-dependent *in vivo* reprogramming of astrocytes was unclear. Furthermore, the subtypes of iANB-derived neurons were not well characterized. In this study, we reveal that SOX2-driven reprogramming of astrocytes transits through intermediate neural progenitor states before the adoption of a mature neuron fate. Immunohistochemistry and electrophysiology further show that induced

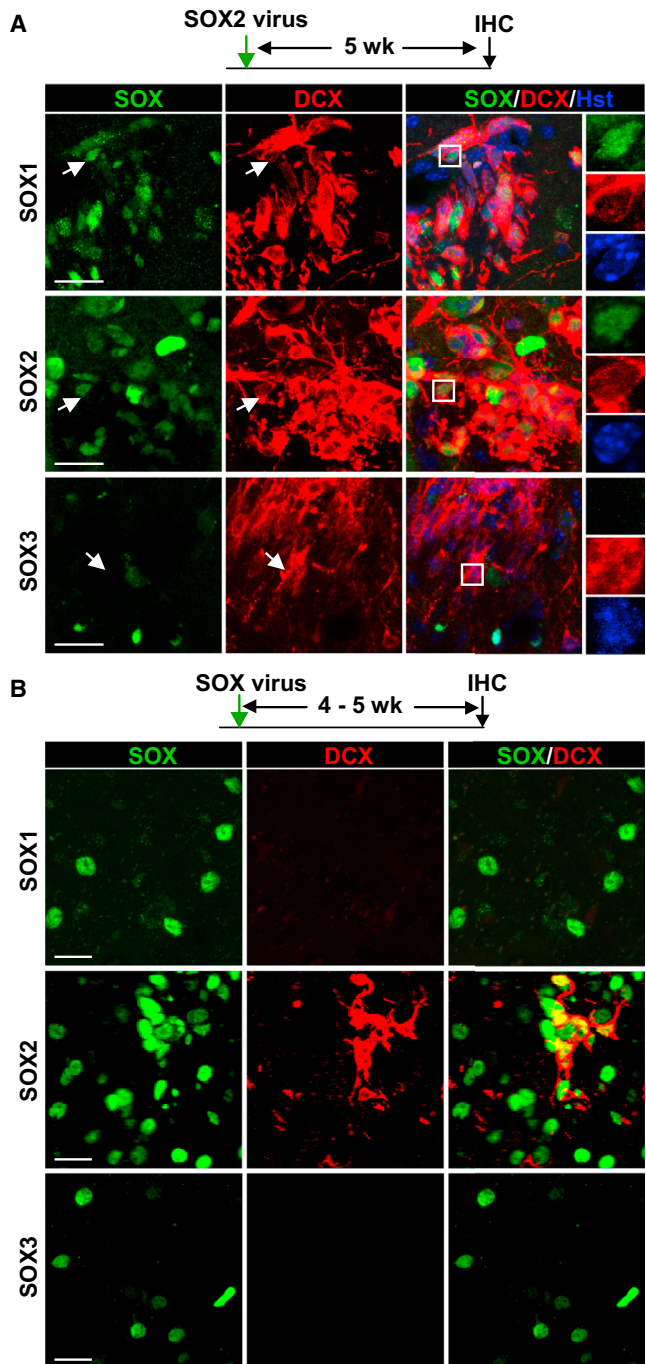


Figure 1. Expression and Reprogramming Ability of SOXB1 Factors

(A) Immunohistochemistry (IHC) showing expression of SOXB1 factors in striatal regions with iANBs at 5 weeks post-injection (wpi) of SOX2 virus. SOX1 and SOX2, but not SOX3, can be identified in some of the induced DCX⁺ cells (right panels at higher magnifications). Hst, Hoechst 33342. The scale bars represent 20 μ m.

(B) Ectopic SOX2, but not the other SOXB1 factors, induce striatal DCX⁺ cells. Lentivirus expressing individual SOXB1 factors was

neurons are functionally mature and predominantly express the marker calretinin.

RESULTS

Ectopic Expression of SOX2, but Not the Other SOXB1 Factors, Results in iANBs

SOX2 belongs to the SOXB1 subfamily of high-mobility group-box transcription factors, which also includes SOX1 and SOX3 (Sarkar and Hochedlinger, 2013). These factors are critical for specifying and maintaining the undifferentiated state of neural precursors. The expression of SOXB1 factors during SOX2-mediated *in vivo* reprogramming were investigated using immunohistochemistry (Niu et al., 2013). The adult mouse striatum was injected with lentivirus expressing SOX2 under the human GFAP promoter. When analyzed 4 weeks post-injection (wpi), DCX⁺ iANBs were robustly detected in the virus-injected regions, confirming our previous results (Niu et al., 2013). Interestingly, SOX1 can also be detected in striatal regions with iANBs, especially in DCX⁺ cell clusters (Figure 1A). However, SOX1 expression is lower in iANBs than neighboring DCX⁻ cells, which is consistent with previous findings that the continued high-level expression of SOXB1 factors prohibits neuronal differentiation (Bylund et al., 2003; Niu et al., 2013). In contrast, SOX3 is only sporadically distributed in the adult striatum and is not detectable in DCX⁺ iANBs (Figure 1A). Due to sequence and potential functional similarity (Bylund et al., 2003), we investigated whether the SOXB1 proteins can similarly induce DCX⁺ cells. Lentiviruses expressing SOX1 or SOX3 under the GFAP promoter were individually injected into the adult striatum. However, when examined at 4 or 5 wpi, no DCX⁺ cells were detected in striatal regions with ectopic SOX1 or SOX3 expression, in sharp contrast to areas injected with SOX2-expressing virus that contain DCX⁺ cells (Figure 1B). Together, these data indicate that SOX2 has a unique property among the SOXB1 factors, enabling the reprogramming of resident astrocytes to iANBs.

SOX2-dependent iANBs in the adult striatum were further examined by injections of lentivirus expressing GFP-T2A-SOX2 under the GFAP promoter (Figure S1). The co-expressed stable GFP marked virus-transduced cells. Immunohistochemical analysis showed that about 23.2% \pm 5.3% of GFP⁺ cells (mean \pm SD; n = 17,841 GFP⁺ cells counted in sections from three mice) stained positive for DCX (Figure S1). This suggests a relatively efficient induction of iANBs from SOX2-expressing cells.

injected into the adult mouse striatum and examined 4 or 5 weeks (wk) later. The scale bars represent 20 μ m. See also Figure S1.



iANBs Are Not the Progeny of Induced Neural Stem Cells

Adult neurogenesis is a multistep process that starts with multipotent neural stem cells (NSCs) that gradually transition into DCX⁺ neuroblasts (Hsieh, 2012; Kempermann et al., 2004; Kriegstein and Alvarez-Buylla, 2009; Ma et al., 2009). Both SOX1 and SOX2 are expressed in NSCs that can give rise to neurons and glia (Suh et al., 2007; Venere et al., 2012). The residual expression of these factors in DCX⁺ iANBs suggests that ectopic SOX2 might reprogram astrocytes into a multipotent NSC state. We surveyed the expression of several additional markers for NSCs surrounding striatal regions injected with SOX2-expressing virus at 4 wpi. Nestin (NES), an intermediate filament protein highly enriched in embryonic and adult NSCs (Lagace et al., 2007), can be sparsely detected in neighboring regions with iANBs (Figure S2). Similarly, cells expressing brain-lipid-binding protein, a marker for radial glia in developing brain and type-1 and type-2 neural precursors of the adult dentate gyrus (DG) (Feng et al., 1994; Steiner et al., 2006), are intermingled with iANBs in the adult striatum. GFAP⁺ cells are also found in the vicinity of iANBs (Figure S2). GFAP is robustly induced in reactive astrocytes and also labels NSCs in the adult lateral ventricle (LV) and DG (Doetsch, 2003; Kriegstein and Alvarez-Buylla, 2009; Lie et al., 2004). Although the above markers were not detected in DCX⁺ cells, these data support a hypothesis that iANBs might be derived from SOX2-induced NSCs in the striatum.

We directly examined this hypothesis using a lineage-tracing strategy. When adult *Nes-CreERTM;Rosa-YFP* mice were treated with tamoxifen for 7 days and examined 3 weeks later, DCX⁺ cells in the LV and DG were robustly labeled with the YFP reporter (Figures 2A and 2B). This result confirms that neuroblasts from endogenous NSCs can be specifically traced in this transgenic mouse line (Kuo et al., 2006; Niu et al., 2013). We then injected SOX2-expressing lentivirus into the striatum of adult *Nes-CreERTM;Rosa-YFP* mice, administered tamoxifen at 2 or 3 wpi, and performed immunohistochemistry after another 3 weeks. As internal controls, endogenous neuroblasts in the LV were traced with the marker YFP. In sharp contrast, none of the SOX2-induced DCX⁺ cells in the striatum were YFP labeled, indicating that ectopic SOX2 does not reprogram astrocytes into a NSC-like state (Figures 2C and 2D).

SOX2 Induces ASCL1⁺ Neural Progenitors

ASCL1⁺ neural progenitors precede the development of DCX⁺ neuroblasts during adult neurogenesis (Kim et al., 2011a; Lugert et al., 2012). Very interestingly, ASCL1⁺ cells can be specifically detected in the striatal regions around DCX⁺ iANBs when injected with SOX2, but not a control

virus, at 5 wpi (Figure 3A). A time course analysis further showed that the number of ASCL⁺ cells gradually increases post-injection of SOX2 virus, reaches a peak level around 5 wpi, and persists beyond 14 wpi (Figure 3B). We used the GFAP-GFP marker to label virus-transduced astrocytes in the adult striatum and revealed specific ASCL1 expression in these GFP⁺ cells, which clustered with SOX2-induced DCX⁺ cells (Figure 3C).

The above results suggest that ASCL1⁺ cells might be the precursors of iANBs during SOX2-driven in vivo astrocyte reprogramming. We examined this possibility using *Ascl1-CreER^{T2}* mice, in which the tamoxifen-inducible *CreER^{T2}* was knocked into the endogenous *Ascl1* locus (Kim et al., 2011b). After crossing to mice harboring the Cre-activity-dependent *Rosa-tdTomato* (*tdT*) reporter (Madisen et al., 2010), ASCL1⁺ cells and their progeny can be uniquely traced. These adult mice were injected with a SOX2-expressing or control virus, administered tamoxifen for 7 days starting at 2 wpi, and examined at 6 wpi (Figure 3D). Whereas no *tdT*⁺ cells were detected in striatal regions injected with the control virus, these cells were robustly distributed in regions injected with the SOX2 virus (Figure 3E). Consistent with the hypothesis that iANBs are derived from ASCL1⁺ neural progenitors, over 90% of SOX2-induced DCX⁺ cells could be labeled by *tdT*. Together, these data show that ectopic SOX2 reprograms striatal astrocytes to ASCL1⁺ neural progenitors, which subsequently give rise to DCX⁺ iANBs.

ASCL1 Is Required, but Not Sufficient, for Generation of iANBs

ASCL1 is a neural specific basic helix-loop-helix transcription factor and essential for neurogenesis during early nervous system development (Casarosa et al., 1999; Nieto et al., 2001; Torii et al., 1999). The induction of ASCL1 in the adult striatum suggests that it may be critical for SOX2-driven in vivo reprogramming of astrocytes. To examine this possibility, we used genetically modified mice that contain conditional alleles of *Ascl1* (*Ascl1^{ff}*; Pacary et al., 2011) and a tamoxifen-inducible *CreER^{T2}* transgene under the astrocyte-specific *Cst3* promoter (Figure 4A) (Niu et al., 2013). These adult mice were treated with tamoxifen or vehicle for 7 days and then injected with SOX2-expressing lentivirus. Immunohistochemistry was performed 5 wpi and revealed a dramatic reduction in the population of DCX⁺ iANBs upon inducible deletion of *Ascl1* (Figures 4B and 4C). The few residual DCX⁺ cells might be due to an incomplete deletion of *Ascl1* in all the SOX2 virus-infected astrocytes. These data indicate that ASCL1 plays a critical role in SOX2-driven reprogramming.

Ectopic ASCL1 is sufficient to promote the neuronal differentiation of embryonic stem cells and NSCs (Berninger et al., 2007; Chanda et al., 2014), as well as reprogram

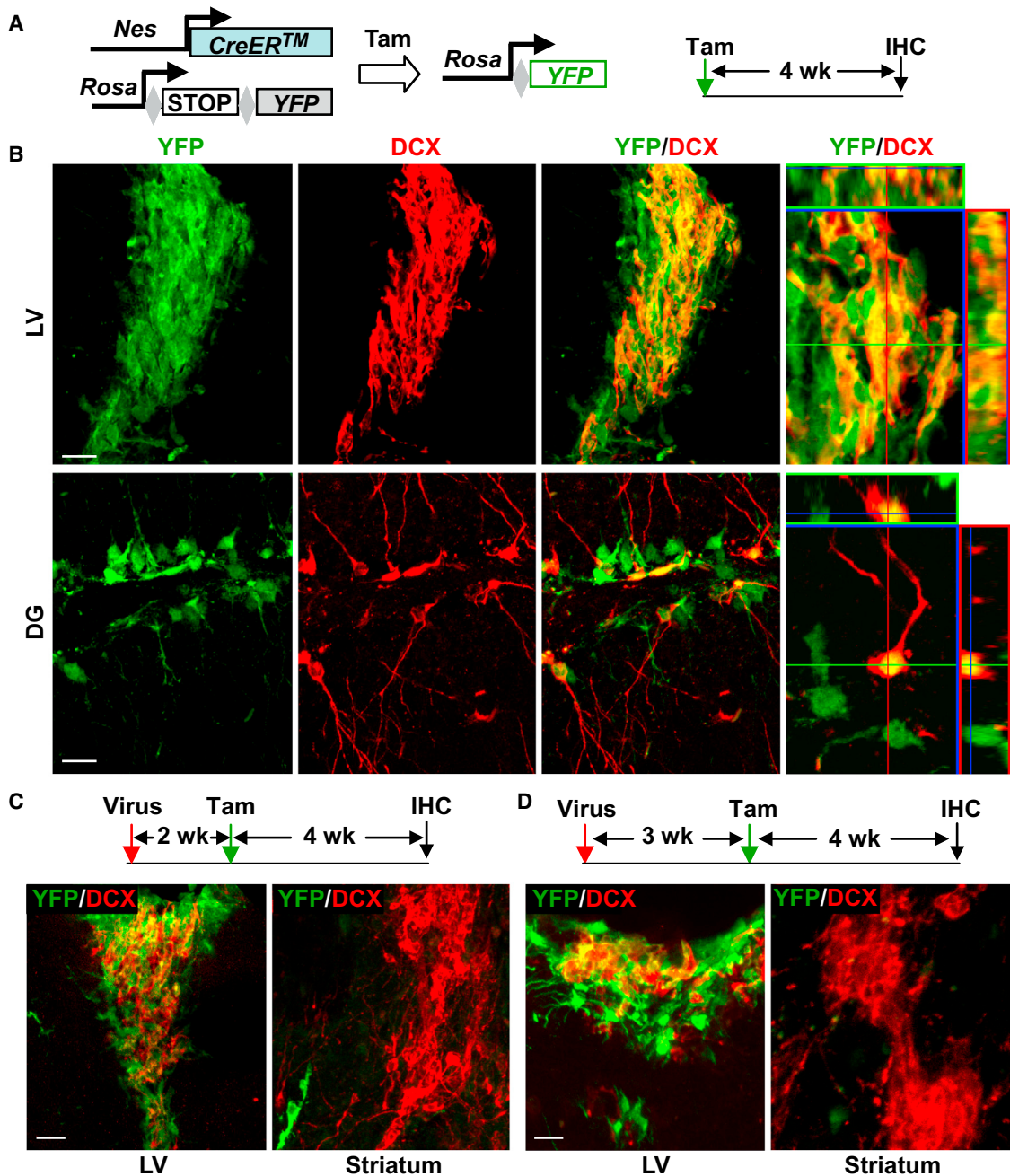


Figure 2. SOX2-Driven Reprogramming Does Not Pass through a NSC Stage

(A) A genetic approach to trace NSCs and their progeny. Adult *Nes-CreERTM;Rosa-YFP* mice were injected with tamoxifen (Tam) for 7 days and examined 3 wk later.

(B) Endogenous NSCs and DCX⁺ cells in the lateral ventricle (LV) and dentate gyrus (DG) are genetically traced. The scale bars represent 20 μ m.

(C and D) iANBs do not pass through a nestin⁺ NSC stage. Adult mutant mice were treated with Tam 2 (C) or 3 (D) wpi of SOX2-expressing virus and examined at the indicated time points. DCX⁺ cells in the LV were used as endogenous controls. The scale bars represent 20 μ m. See also Figure S2.

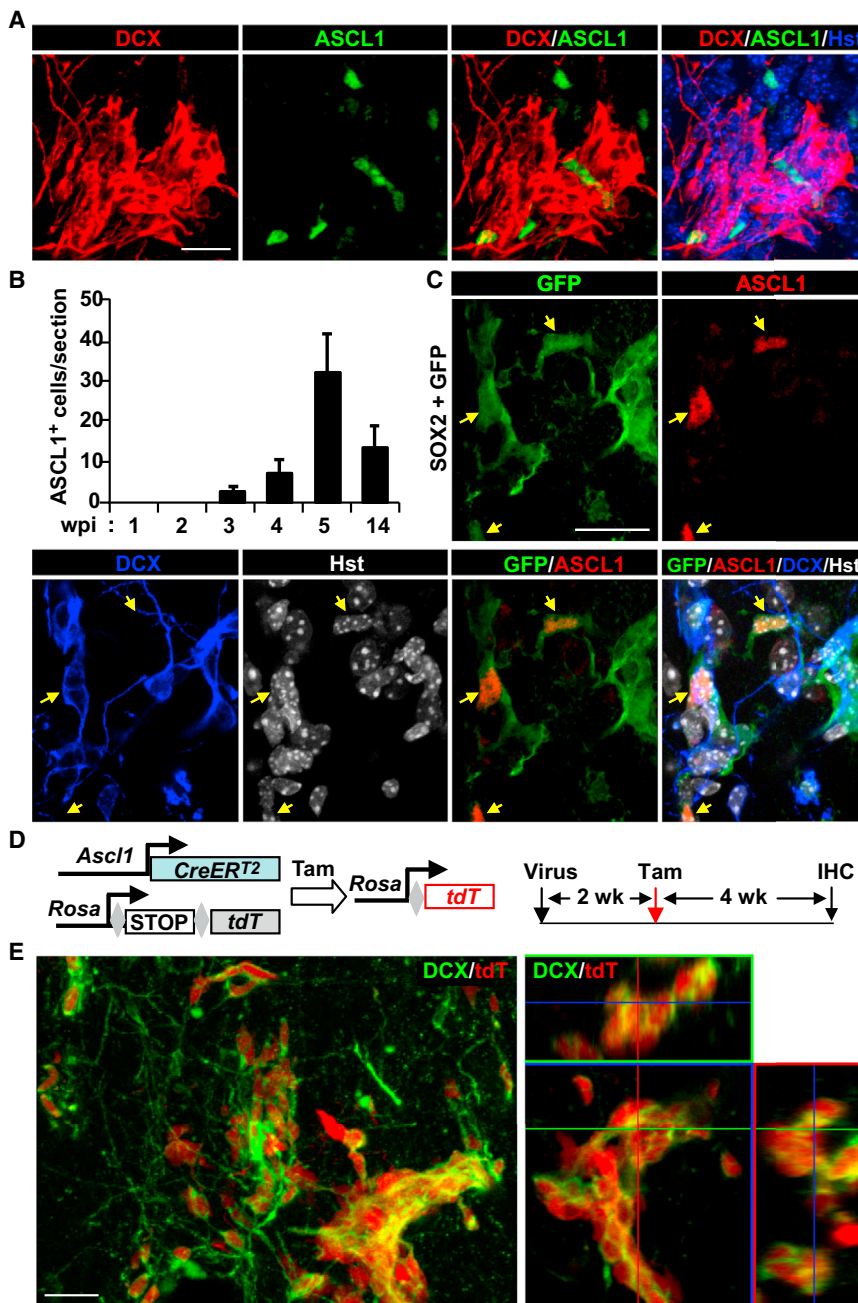


Figure 3. SOX2 Induces ASCL1⁺ Neural Progenitors

(A) The expression of ASCL1⁺ cells in striatal regions with DCX⁺ iANBs at 5 wpi. The scale bar represents 20 μ m.

(B) A time course analysis of ASCL1⁺ cells in the reprogramming area (mean \pm SD; n = 3 mice at each time point).

(C) ASCL1 is detected in astrocytes transduced with SOX2 lentivirus. The co-expressed GFP marker is under the control of the human GFAP promoter. The scale bar represents 20 μ m.

(D) A genetic approach to trace derivatives of ASCL1⁺ progenitors. SOX2-driven reprogramming was induced in adult *Ascl1-CreERT2*; *Rosa-tdTomato* (tdT) mice.

(E) SOX2-induced DCX⁺ cells pass through an ASCL1⁺ progenitor stage. Confocal images show genetic labeling of iANBs. An orthogonal view is shown in the right panel. The scale bar represents 20 μ m.

cultured fibroblasts and early postnatal astroglia to neurons (Chanda et al., 2014; Heinrich et al., 2011), demonstrating a dominant role for ASCL1 in cell fate specification. To investigate whether ASCL1 itself is also able to induce DCX⁺ neuroblasts in the adult striatum, we injected lentivirus expressing ASCL1 under the GFAP promoter and analyzed 1, 2, 3, and 5 wpi (Figure 4D). Unexpectedly, DCX⁺ cells were not observed in regions with robust expression of exogenous ASCL1 (Figure 4E). These results suggest that ASCL1 has important roles in the SOX2-driven

reprogramming process but is not itself sufficient to induce cell fate switch in the adult striatum.

iANBs Mostly Generate Calretinin⁺ Interneurons

We previously showed that iANBs can give rise to functionally mature neurons upon treatment with brain-derived neurotrophic factor (BDNF) and noggin or with the small molecule valproic acid (VPA) (Niu et al., 2013). However, the subtype of neurons generated by these treatments was unclear. We surveyed the expression of markers for

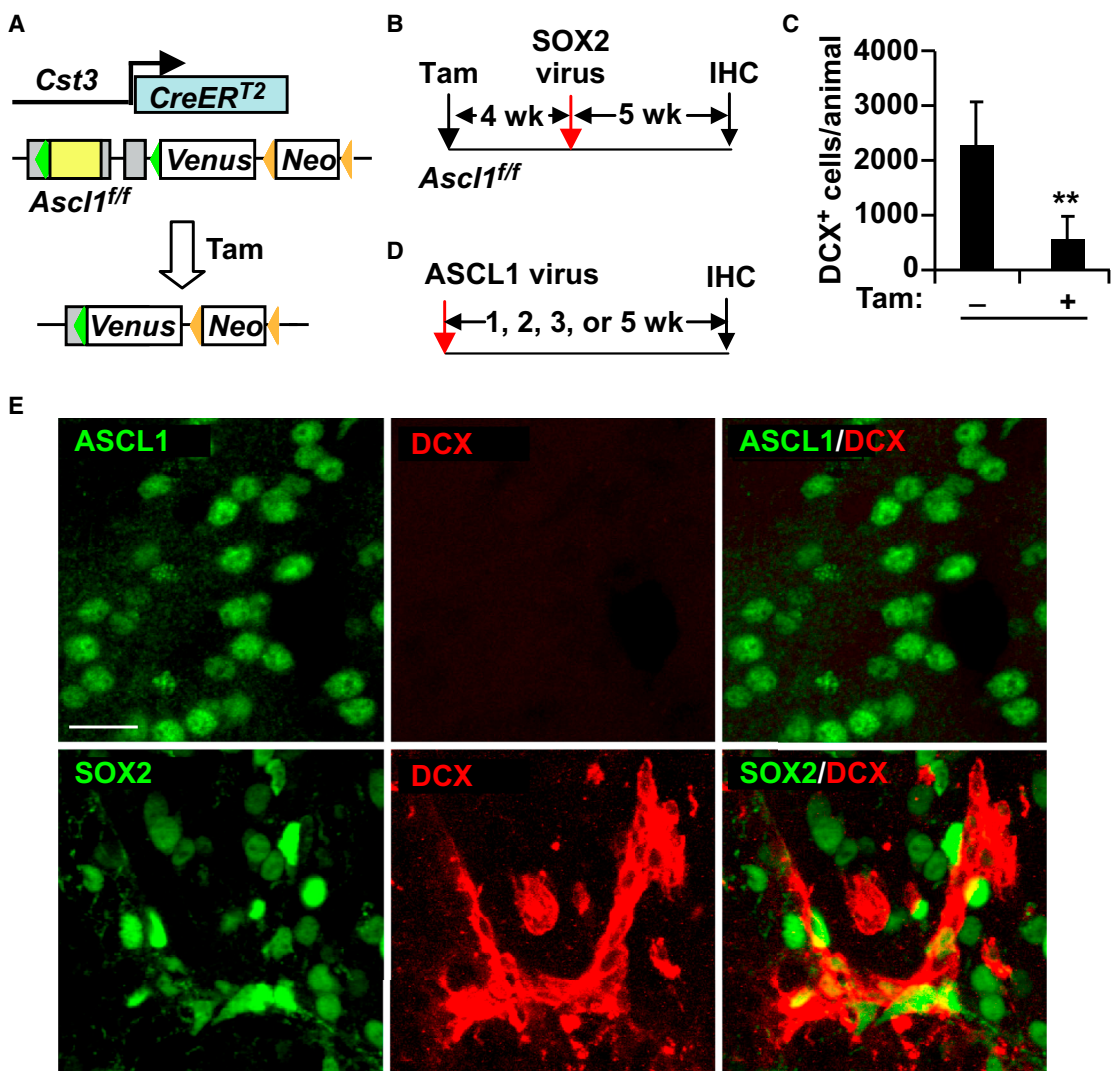


Figure 4. ASCL1 Is Required, but Not Sufficient, for SOX2-Driven Reprogramming

(A and B) Schematic diagrams show experimental designs. *Ascl1* is deleted in the adult astrocytes after Tam treatment of *Ascl1^{ff}*; *Cst3-CreER^{T2}* mice. Four weeks later, in vivo reprogramming was initiated by injection of SOX2-expressing lentivirus and examined at 5 wpi. (C) Deletion of *Ascl1* dramatically reduces the induction of DCX⁺ cells (mean ± SD; n = 6 for vehicle-treated and n = 4 for Tam-treated mice; **p = 0.0013 by Student's t test).

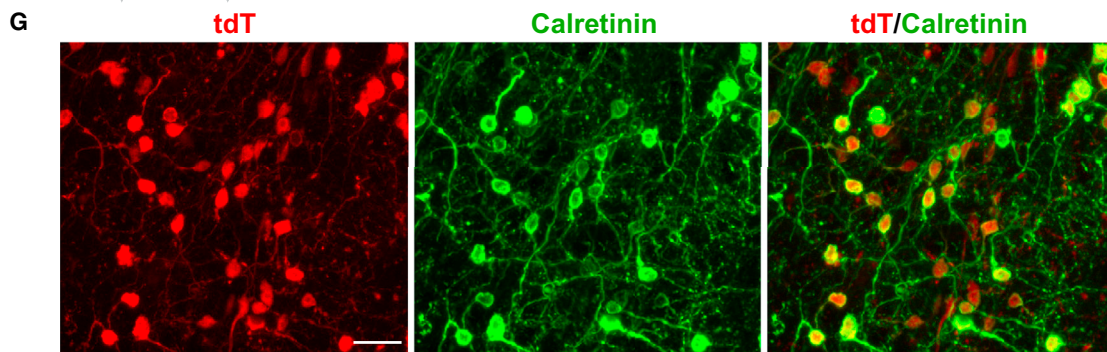
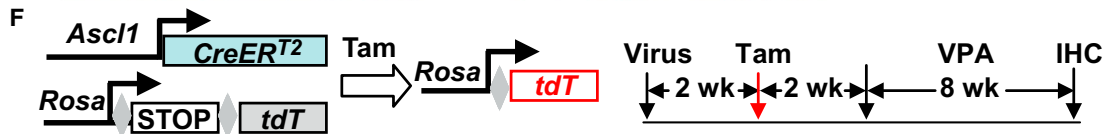
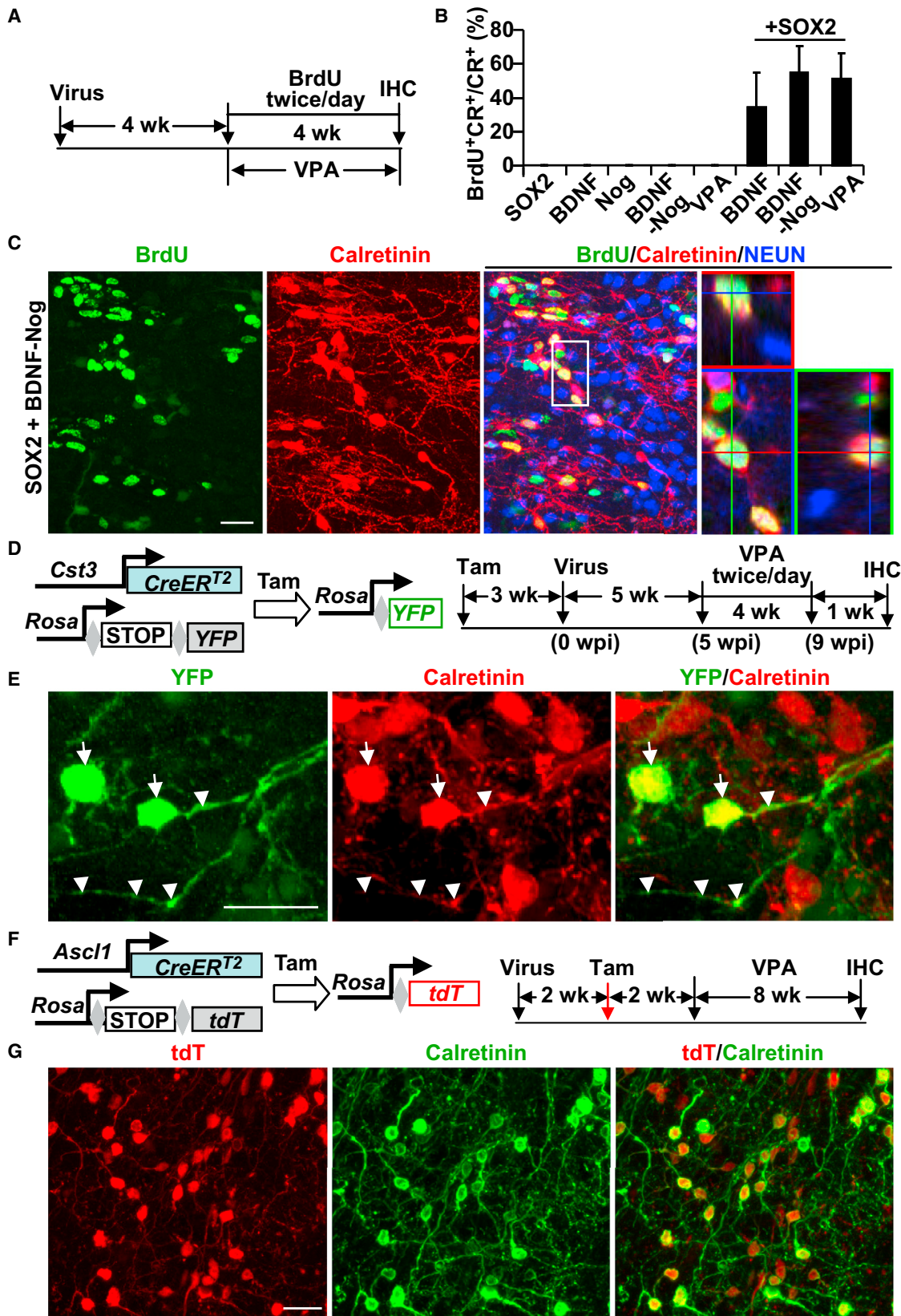
(D) The experimental design for examining ASCL1 reprogramming ability.

(E) DCX⁺ cells were not detected in striatal regions with ectopic ASCL1 when examined at 1, 2, 3, or 5 weeks post virus injection. SOX2-induced DCX⁺ cells were used as positive controls. The scale bar represents 20 μm.

striatal neurons by immunohistochemistry in regions injected with SOX2 virus at 8 wpi. To promote neuron survival and maturation, some of these mice were also injected with virus expressing BDNF or BDNF-noggin or were treated with VPA for 4 weeks starting at 4 wpi (Figures S3A and S3B). Among all these treatment groups, we did not notice any major change in the populations of neurons expressing parvalbumin, somatostatin, choline acetyltransferase, tyrosine hydroxylase, or DARPP32 (Figure S3C; data not shown). In sharp contrast, we observed a dramatic

induction of calretinin neurons in striatal regions of mice injected with SOX2 virus and treated with the neurotrophic factors or small molecule (Figures S3C and S3D). This combination treatment was essential for the induction of calretinin neurons, as they were not observed in mice injected with only virus or treated with only VPA.

We performed bromodeoxyuridine (BrdU) tracing to confirm these calretinin neurons were indeed newly induced. Adult mice were injected singularly or in combination with viruses expressing SOX2, BDNF, noggin, or



(legend on next page)



BDNF-noggin. A cohort of SOX2 virus-injected mice was also treated with VPA in drinking water for 4 weeks beginning at 4 wpi. All mice were administered BrdU for 4 weeks to label newly generated cells (Figure 5A). When analyzed at 8 wpi, 30%–70% of calretinin cells could be traced by BrdU in striatal regions injected with SOX2 virus and treated with either neurotrophic factors or VPA (Figure 5B). A majority of these BrdU⁺ calretinin⁺ neurons were also NEUN⁺, a marker for mature neurons (Figure 5C). These neurons were not detectable in any of the control groups, confirming that the long-term survival and maturation of SOX2-induced neurons requires neurotrophic factors (Niu et al., 2013).

Cell-of-origin tracing was used to map the lineage of induced calretinin⁺ neurons in transgenic mice. Astrocytes were specifically labeled by tamoxifen-inducible expression of YFP in adult *Cst3-CreER^{T2};Rosa-YFP* mice (Figure 5D) (Niu et al., 2013). Three weeks later, these mice received striatal injections of SOX2-expressing lentivirus and were treated with VPA for 4 weeks starting at 5 wpi. When analyzed at 10 wpi, calretinin⁺ neurons were uniquely traced by YFP, indicating an origin from adult striatal astrocytes (Figure 5E). However, not all calretinin⁺ neurons were YFP⁺, a result that might be due to the incomplete labeling of striatal astrocytes by the inducible approach and a few preexisting endogenous calretinin⁺ neurons.

Ascl1-CreER^{T2};Rosa-tdT mice were employed to further examine whether SOX2-induced calretinin⁺ neurons pass through an ASCL1⁺ intermediate progenitor stage (Figure 5F). These adult mice were first injected with SOX2-expressing lentivirus to induce reprogramming and treated with tamoxifen at 2 wpi to label cells derived from ASCL1⁺ progenitors. When examined at 6 wpi, many of the calretinin⁺ interneurons were tdT⁺ (Figure 5G), indicating that they were indeed derived from SOX2-induced ASCL1⁺ progenitors. As controls, calretinin⁺ tdT⁺ cells were not detectable in striatal regions injected with GFP-ex-

pressing lentivirus. The long-term survival of SOX2-induced neurons was determined at 36 wpi (Figure S3E). About 94.6% ± 0.9% tdT⁺ cells (mean ± SD; n = 369 tdT⁺ cells from three mice) were NeuN⁺, indicating that a majority of the induced neurons become mature and exhibit long-term survival in the endogenous environment (Figure S3F).

Functional Heterogeneity of Induced Neurons

We conducted whole-cell patch clamp recordings on reprogrammed striatal neurons using live brain slices from adult *Ascl1-CreER^{T2};Rosa-tdT* mice. Mice at 2–4 months of age were injected with SOX2-expressing lentivirus to initiate the reprogramming of astrocytes and 2 weeks later treated with tamoxifen for 7 days to trace induced neurons. To promote the survival and maturation of induced neurons, mice were also treated with VPA for at least 4 weeks starting at 4 wpi. Electrophysiology was performed from 8 to 40 wpi. The morphology of recorded cells was visualized by the infusion of biocytin through recording pipettes (Figure 6A).

Based on resting membrane potential and input resistance, the induced neurons can be broadly grouped into four subtypes (Figures 6B–6D). The vast majority of the induced neurons (type I; n = 20/27) exhibit hyperpolarized resting membrane potential at –80 mV and have a lower input resistance (30–80 MΩ). Type II neurons (n = 2/27) are similarly hyperpolarized around –80 mV but show a much-higher input resistance (200–1,000 MΩ). The resting membrane potential of type III (n = 2/27) and type IV (n = 3/27) neurons is –60 mV; however, the respective input resistances differ widely, ~150 MΩ and ~2,000 MΩ. Cell capacitance, which usually serves as an indicator of cell size and channel abundance on the membrane, varies broadly among these recorded neurons (Figure 6E).

Functional maturity was examined by the ability to fire action potentials (APs), which were elicited by a series of

Figure 5. Reprogramming of Resident Astrocytes to Calretinin⁺ Neurons

- (A) Experimental schemes. Newly generated cells were labeled by BrdU incorporation. Neuronal survival and maturation were promoted by valproic acid (VPA) or neurotrophic factors.
- (B) Quantification of newly generated calretinin (CR)⁺ neurons under the indicated conditions (mean ± SD; n = 3 mice at each condition). BDNF, brain-derived neurotrophic factor; Nog, noggin.
- (C) Confocal images showing BrdU-labeled CR⁺ neurons that were induced by SOX2. An orthogonal view of the boxed region is also shown. The scale bar represents 20 μm.
- (D and E) SOX2-induced CR⁺ neurons originate from resident astrocytes. Adult resident astrocytes were genetically traced in *Cst3-CreER^{T2};Rosa-YFP* mice after Tam treatment. These cells were then in vivo reprogrammed by ectopic SOX2 and analyzed 10 weeks later. Soma and processes of the astrocyte-converted CR⁺ neurons are indicated by arrows and arrowheads, respectively. The scale bar represents 20 μm.
- (F and G) SOX2-induced CR⁺ neurons pass through an ASCL1 progenitor stage. The descendants of ASCL1⁺ progenitors were genetically traced in *Ascl1-CreER^{T2};Rosa-tdT* mice. A majority of the reprogrammed CR⁺ neurons were traced by the marker tdT. The scale bar represents 20 μm.

See also Figure S3.

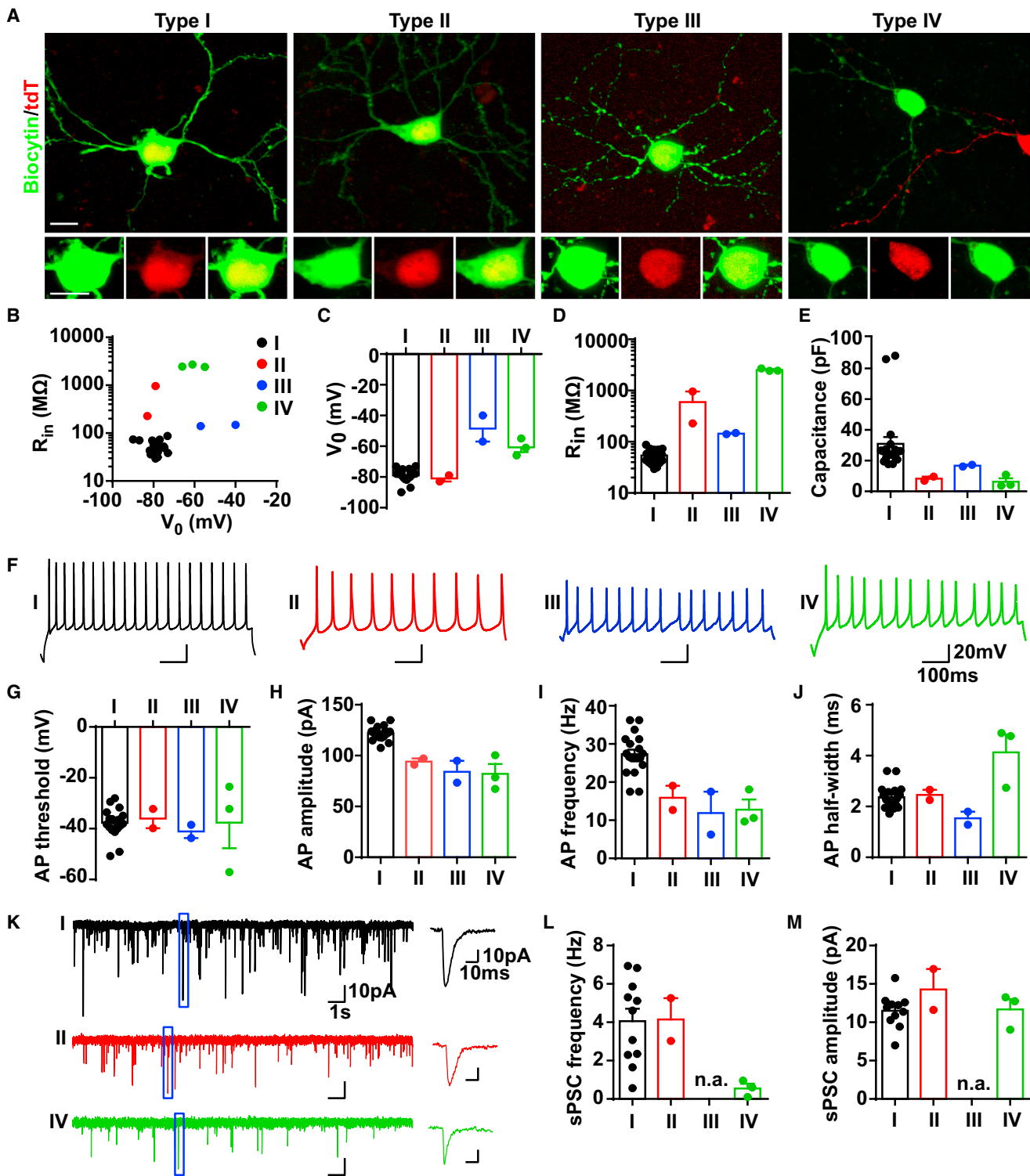


Figure 6. Functional Properties of SOX2-Induced Neurons

(A) Representative confocal images of the four types of induced neurons traced in the striatum of adult *Ascl1-CreER^{T2};Rosa-tdT* mice and infused with biocytin. The scale bars represent 10 μ m.
(B–D) Characterization of the four types of induced neurons based on input resistance (R_{in}) and resting membrane potentials (V_0).
(E) A majority of the recorded neurons have a capacitance around 30 pF.

(legend continued on next page)

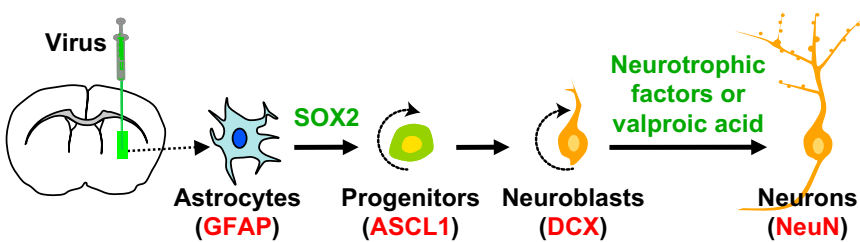


Figure 7. Stepwise Reprogramming of Resident Astrocytes to Functional Neurons in the Adult Brain

current-step injections. All induced neurons fired repetitive APs when depolarized beyond the AP threshold ($n = 27/27$; Figures 6F and S4A). Although the AP threshold (Figure 6G) and delay of the first AP spike (Figure S4B) were within a broad range, type I neurons exhibited larger amplitudes and higher firing frequencies ($n = 20$; Figures 6H and 6I). On the other hand, type IV induced neurons had a wider AP half-width (Figure 6J) and slower velocity of AP rise and decay ($n = 3$; Figures S4C and S4D). Interestingly, type III induced neurons spontaneously fired APs at their resting membrane potential (Figures S3E and S4F), a phenomenon widely observed in many CNS neurons. These neurons might function in the synchronization of circuit activity or sustain modulatory inputs onto postsynaptic neurons (Häusser et al., 2004; Maccaferri and McBain, 1996).

By depolarizing the induced neurons from -60 mV to $+60$ mV in 10-mV increments, we further examined the behaviors of sodium and potassium channels (Figure S4G). The large inward current from voltage-gated sodium channels was completely blocked by the application of tetrodotoxin (Figure S4H). These sodium currents (I_{Na}) varied broadly and were not considerably different between subtypes of induced neurons (Figure S4I). The outward currents in the plateau phase of the voltage step represent delayed rectifier potassium currents (I_d ; Figure S4G), which were much lower in type IV induced neurons (Figure S4J). The approximate summation of fast potassium current (I_A) and I_d collectively represent the outward current immediately following the inward sodium current. I_A was smaller in type IV induced neurons than the other three types (Figure S4K). These data suggest that ion channel distributions in type IV induced neurons are different from the other three types.

- (F) Representative action potential traces from each type of reprogrammed neurons.
 - (G) All the induced neurons have a similar action potential (AP) threshold.
 - (H and I) A majority of the induced neurons have higher AP amplitudes and frequencies.
 - (J) Type IV induced neurons have wider AP half-width.
 - (K–M) Properties of spontaneous postsynaptic currents (sPSCs). Whereas there is a broader range of sPSC frequencies, their amplitude is rather similar (n.a., not available).
- For all panels, $n = 20$ cells from 11 mice for type I neurons, $n = 2$ cells from two mice for type II neurons, $n = 2$ cells from one mouse for type III neurons, and $n = 3$ cells from three mice for type IV neurons.
See also Figure S4.

Neuron connectivity within the local circuitry was investigated by recording spontaneous postsynaptic currents (sPSCs). All of the analyzed neurons showed robust sPSCs with comparable average amplitudes, although the frequency was lower in type IV induced neurons (Figures 6K–6M). These results indicate that all of the induced neurons have efficiently integrated into the local neuronal networks and received inputs from presynaptic neurons.

DISCUSSION

This study used genetic fate mapping to reveal that SOX2-driven *in vivo* reprogramming of adult astrocytes passes through a sequence of distinct cell states (Figure 7), which mimics aspects of endogenous neurogenesis. Ectopic SOX2 converts astrocytes to ASCL1⁺ intermediate progenitors, which proliferate and generate DCX⁺ neuroblasts. These early neuroblasts can expand and eventually generate mature neurons when supplied with neurotrophic factors. Expansion through the intermediate progenitors and neuroblasts enable one reprogrammed astrocyte to make multiple functional neurons, which might be therapeutically beneficial for regenerative medicine in treating neural injuries or degeneration.

Although previous work showed that SOX2 is sufficient to convert fibroblasts into NES⁺ multipotent NSCs under a unique culture condition (Ring et al., 2012), our genetic approach using *Nes-CreER^{T2};Rosa-YFP* mice failed to detect a stable NSC state during the *in vivo* reprogramming process. This difference highlights the critical importance of the microenvironment in cell fate reprogramming and suggests that additional factors are required to enable SOX2 to convert glial cells into multipotent stem cells in the adult



CNS. Our initial *in vivo* screens for reprogramming factors included the four factors for induced pluripotent stem cells (Niu et al., 2013); however, this combination of factors has been subsequently shown to induce tumorigenesis *in vivo* (Abad et al., 2013; Ohnishi et al., 2014) and raised serious concerns about the therapeutic value of *in vivo* induced pluripotent stem cells. In contrast, we have not observed any histological signs of tumorigenesis in brains or spinal cords with ectopic SOX2 expression when examined up to 1 year post virus injection. This is consistent with a recent study showing that multiple key transcription factors are required to initiate brain tumors *in vivo* (Suvà et al., 2014).

Adult neurogenesis is a multistep process beginning with multipotent NSCs that yield transient amplifying neural progenitors and then mature neurons (Gage, 2000; Hsieh, 2012; Kriegstein and Alvarez-Buylla, 2009; Lie et al., 2004). Our immunohistochemistry and genetic fate-mapping experiments demonstrate that SOX2-driven *in vivo* reprogramming passes through an ASCL1⁺ intermediate progenitor stage. These progenitors give rise to DCX⁺ neuroblasts, which can further proliferate and expand the neuronal lineage (Niu et al., 2013). This sequential and multistage amplification process is consistent with what has been observed in the adult neurogenic niches, suggesting that the reprogrammed glial cells have adopted the behavior of endogenous progenitors (Kim et al., 2011b; Lügert et al., 2012). ASCL1 serves as a molecular marker of neural progenitors and also controls their activity, including proliferation and differentiation (Andersen et al., 2014; Battiste et al., 2007; Jessberger et al., 2008; Kim et al., 2007, 2008). Consistently, our conditional deletion of *Ascl1* in astrocytes shows that it is critically important for robust *in vivo* reprogramming. Nonetheless, ASCL1 cannot replace SOX2 in the induction of neurogenesis from adult astrocytes, as DCX⁺ iANBs are rarely detected in striatal regions with ectopic ASCL1 during a series of time course analyses. This result agrees with a recent *in vivo* study (Heinrich et al., 2014) and suggests that additional factors are also required in combination with ASCL1 to mediate SOX2 function in cell fate reprogramming in the adult brain. In contrast, ASCL1 alone is able to transdifferentiate early postnatal astroglia (Heinrich et al., 2010, 2012), fibroblasts (Chanda et al., 2014), and embryonic stem cells (Chanda et al., 2014) into functional neurons in culture. This discrepancy between results from *in vitro* and *in vivo* studies once again highlights the importance of the cellular milieu in cell fate specification, determination, and reprogramming.

A survey of markers for neuronal subtypes reveals that a larger population of SOX2-induced neurons expresses calretinin, a calcium-binding protein in GABAergic interneurons (Tepper et al., 2010). Interestingly, calretinin was shown to be transiently co-expressed with DCX during

the early stage of adult hippocampal neurogenesis and subsequently downregulated once newly born neurons become mature 6 weeks later (Brandt et al., 2003). In contrast, calretinin is rarely detectable in iANBs but continuously expressed once they develop into mature neurons by 8 wpi, suggesting the stable generation of this neuronal subtype. The preferential reprogramming of striatal astrocytes by SOX2 to calretinin⁺ neurons was unexpected but is most likely due to signaling cues present in the adult striatum or intrinsic factors residing in the striatal astrocytes. It will be interesting in the future to tease out these instructive factors for the generation of specific neuron subtypes.

Endogenous calretinin⁺ interneurons make up 0.5% of striatal neurons in the rodent but are more prevalent in humans (Rymar et al., 2004; Wu and Parent, 2000). These neurons are diverse in morphology with limited electrophysiological characterization (Tepper et al., 2010). Electrophysiological analyses show that the induced neurons are heterogeneous, although the majority is hyperpolarized with lower input resistance and higher AP amplitude and frequency. This heterogeneity may reflect functional diversity and/or the progressive nature of neuronal maturation and integration into the local circuits. Interestingly, a minority of the recorded neurons exhibit pacemaker-like activity and fire spontaneous APs at resting membrane potential. This activity is prevalent in striatal cholinergic neurons, subthalamic nucleus neurons, midbrain dopaminergic neurons, cerebellar Purkinje and Golgi neurons, and low-threshold spike interneurons of the striatum (Beatty et al., 2012; Reynolds and Wickens, 2004; Sharott et al., 2012). The pace-making activity of these neurons can synchronize neuronal networks for higher-order brain functions (Ramirez et al., 2004).

The ability to reprogram glial cells into functional neurons in the adult CNS has reshaped our knowledge of cell fate maintenance and brought a new perspective to cell-based regenerative medicine for neurological diseases. The results of this study provide new insights into the cellular processes of SOX2-driven *in vivo* reprogramming, which may be useful for future strategies aimed at improving reprogramming efficiency and the derivation of disease-relevant neuron subtypes.

EXPERIMENTAL PROCEDURES

Animals

The following mutant mouse lines were used in this study: *Cst3-CreER^{T2}* (Niu et al., 2013), *Nes-CreERTM* (Kuo et al., 2006), *Ascl1-CreER^{T2}* (Kim et al., 2011b), *Ascl1^{neoflox/neoflox}* (floxed allele of *Ascl1* mutant mice with the *neo* cassette, here referred to as *Ascl1^{ff}*; Pacary et al., 2011), *Rosa-YFP* (Srinivas et al., 2001), and *Rosa-tdTomato* (Ai14; Rosa-*tdT*; Madisen et al., 2010).



Adult male and female mice at 2–6 months of age were used unless otherwise stated. All mice were housed under a 12 hr light/dark cycle and had ad libitum access to food and water in a controlled animal facility. Experimental protocols were approved by the Institutional Animal Care and Use Committee at UT Southwestern.

Tamoxifen, VPA, and BrdU Administration

Tamoxifen (T5648; Sigma) was dissolved in a mixture of ethanol and sesame oil (10:90 by volume) at a concentration of 40 mg/ml and stored at 4°C. It was intraperitoneally injected at a daily dose of 4 mg/40 g body weight daily for 5–7 days. VPA (P4543; Sigma) in drinking water (4 g/l) was administered for 4 weeks. BrdU (B5002; Sigma; 10 mg/kg body weight in PBS) was applied by daily intraperitoneal injection for 4 weeks.

Virus Preparation and Intracerebral Injections

The lentiviral vectors *GFAP-GFP*, *GFAP-SOX2*, *GFAP-GFP-T2A-SOX2*, *GFAP-GFP-T2A-Bdnf*, and *GFAP-GFP-T2A-Noggin* were generated as previously described (Niu et al., 2013). A final volume of 2 μ l virus with an original titer of 0.5–1 \times 10⁹ colony-forming units per ml was stereotactically injected into the striatum of adult mice with a coordinate of anterior/posterior, +1.0 mm; medial/lateral, \pm 2 mm; and dorsal/ventral from skull, −3.0 mm.

Immunohistochemistry

Adult mice were euthanized with CO₂ overdose and sequentially perfused with ice-cold PBS and 4% paraformaldehyde (PFA) in PBS. Brains were collected and postfixed with 4% PFA for 4–6 hr or overnight at 4°C. Postfixed brains were cryoprotected with 30% sucrose solution in PBS for 24 hr and cut into 40- μ m-thick sections with a sliding microtome (Leica). Brain sections were serially collected and stored in antifreezing solution at −20°C. Immunohistochemistry was performed essentially as previously described (Niu et al., 2011). Briefly, free-floating sections were rinsed with PBS and blocked with blocking solution (3% BSA and 0.2% Triton X-100 in PBS) for 1 hr at room temperature. These sections were incubated with primary antibodies diluted in blocking solution for at least 24 hr at 4°C followed by three rinses with PBST buffer (0.2% Triton X-100 in PBS). They were subsequently incubated with respective secondary antibodies diluted in blocking solution for over 2 hr at room temperature. Nuclei were counterstained with Hoechst 33342 when appropriate. After extensive rinsing with PBST buffer, sections were mounted onto glass slides for microscopy. The following primary antibodies were used: GFP (A-11122, rabbit, 1:500, Invitrogen; GFP, chick, 1:1,000, Aves Labs), GFAP (G3893; mouse, 1:500; Sigma), BrdU (OBT0030; rat BU1/75; 1:500; Accurate Chemical), NEUN (MAB377; mouse, 1:500; Millipore), SOX1 (4194S; rabbit, 1:500; Cell Signaling Technology), SOX2 (AB5603; rabbit, 1:500; Millipore), SOX3 (rabbit, 1:200; a gift from M. Klymkowsky; Wang et al., 2006), BLBP (AB9558; rabbit, 1:500; Millipore), NES (556309; mouse, 1:200; BD PharMingen), KI-67 (NCL-Ki67; rabbit, 1:500; Novocastra), DCX (sc-8066; goat, 1:150; Santa Cruz Biotechnology), OLIG2 (AB9610; rabbit, 1:500; Millipore), glutamine synthetase (MAB302; mouse, 1:500; Chemicon), PSA-NCAM (5A5-a; mouse, 1:250; Hybridoma bank), NG2 (MAB5384; mouse, 1:500; Milli-

pore), IBA1 (019-19741; rabbit, 1:1,000; Waco), Parvalbumin (P3088; mouse, 1:1,000; Sigma), somatostatin (AB5494; rabbit, 1:500; Chemicon), CHAT (CAT; chick, 1:1,000; Aves), Calretinin (AB702; rabbit, 1:200; Novus), DARPP32 (2302; rabbit, 1:500; Cell Signaling Technology), CC-1 (OP80; mouse, 1:500; Calbiochem), and ASCL1 (TX-518; guinea pig, 1:10,000; Jane Johnson). Alexa-488-, Alexa-Fluor-594-, or Alexa-Fluor-647-conjugated corresponding secondary antibodies from Jackson ImmunoResearch were used for indirect fluorescence. Images were taken using a Zeiss LSM510 confocal microscope. A Cell Counter software plugin in the ImageJ program was used to count cells. Data were obtained from 12 random sections from three to five mice in each group.

Electrophysiology

Adult mice were deeply anesthetized and transcardially perfused with chilled (4°C) artificial cerebrospinal fluid (ACSF) (119 mM NaCl, 2.5 mM KCl, 26 mM NaHCO₃, 1 mM NaH₂PO₄, 11 mM D-glucose at pH 7.4, 300 mOsm, and aerated with 95% O₂/5% CO₂), including 0.5 mM CaCl₂, 5 mM MgCl₂, and 1% kynureneate acid. The striatum with overlying neocortex was then dissected out. Acute sagittal slices (250 μ m thickness) were collected between +2 mm and −2 mm from bregma on a Leica VT1200S slicer. They were then incubated in aerated ACSF with 3 mM CaCl₂ and 2 mM MgCl₂ to recover for 30 min at 35°C followed by additional incubation for over 1 hr at room temperature. A single slice was then transferred to a submersion chamber and perfused at 3 ml/min with aerated ACSF at 30°C. Lineage-traced cells in the striatum were identified under visual guidance using IR-DIC optics and tdTomato fluorescence. Whole-cell current-clamp and voltage-clamp recordings were performed using glass pipettes (\sim 6–9 M Ω) filled with intracellular solution (0.2 mM EGTA, 130 mM K-gluconate, 6 mM KCl, 3 mM NaCl, 10 mM HEPES, 4 mM ATP-Mg, 0.4 mM GTP-Na, and 14 mM phosphocreatine-Tris at pH 7.2 and 285 mOsm). Intracellular solution was supplemented with 0.5% biocytin (B4261; Sigma) for biocytin labeling. All recordings were obtained with a MultiClamp 700B amplifier. Currents were filtered at 2 kHz, acquired, and digitized at 10 kHz using Clampex10.3 (Molecular Devices). APs were recorded in current clamp mode and elicited by a series of current injections starting from −160 pA with 20-, 40-, 80-, or 160-pA increments and 800 ms duration. Sodium and potassium currents were recorded in voltage-clamp mode in response to a series of voltage steps ranging from −60 mV to +60 mV at 10-mV increments and 100 ms duration. Delayed rectifier potassium currents (K_d) were measured 50 ms prior to the end of current step. Spontaneous synaptic currents were recorded in voltage-clamp mode. In all voltage-clamp recordings, cells were clamped at −60 mV or −80 mV, whichever is close to the resting membrane potential of the cell except during the voltage-step protocol. In all current-clamp recordings, recordings were made at the resting membrane potential or without any current injection. Series and input resistance were measured in voltage-clamp mode with a 400 ms, −10 mV step from a −60 mV holding potential (filtered by 10 kHz, sampled at 50 kHz). Cells were accepted only if the series resistance was less than 30 M Ω and stable throughout the experiment. Data analysis was performed in Clampfit10.3 (Molecular Devices).



SUPPLEMENTAL INFORMATION

Supplemental Information includes four figures and can be found with this article online at <http://dx.doi.org/10.1016/j.stemcr.2015.03.006>.

AUTHOR CONTRIBUTIONS

W.N., T.Z., and C.-L.Z. conceived and designed the experiments. W.N. and T.Z. performed the experiments. Y.Z. maintained mouse colonies. D.K.S., T.Y.V., R.B., and J.E.J. provided critical reagents and comments. W.N., T.Z., and C.-L.Z. analyzed data and prepared the manuscript.

ACKNOWLEDGMENTS

We thank members of the C.-L.Z. laboratory for discussions and reagents, Dr. F. Guillemot for sharing the *Ascl1^{ff}* mice, and Dr. M. Klymkowsky for SOX3 antibody. C.-L.Z. is a W. W. Caruth, Jr. Scholar in Biomedical Research. This work was supported by the Welch Foundation Award (I-1724), the Ellison Medical Foundation Award (AG-NS-0753-11), Texas Institute for Brain Injury and Repair, the Decherd Foundation, and NIH grants (NS070981 and NS088095 to C.-L.Z. and NS032817 to J.E.J.).

Received: January 20, 2015

Revised: March 24, 2015

Accepted: March 26, 2015

Published: April 23, 2015

REFERENCES

- Abad, M., Mosteiro, L., Pantoja, C., Cañamero, M., Rayon, T., Ors, I., Graña, O., Megías, D., Domínguez, O., Martínez, D., et al. (2013). Reprogramming *in vivo* produces teratomas and iPS cells with totipotency features. *Nature* *502*, 340–345.
- Andersen, J., Urbán, N., Achimastou, A., Ito, A., Simic, M., Ullom, K., Martynoga, B., Lebel, M., Göritz, C., Frisén, J., et al. (2014). A transcriptional mechanism integrating inputs from extracellular signals to activate hippocampal stem cells. *Neuron* *83*, 1085–1097.
- Arlotta, P., and Berninger, B. (2014). Brains in metamorphosis: reprogramming cell identity within the central nervous system. *Curr. Opin. Neurobiol.* *27*, 208–214.
- Battiste, J., Helms, A.W., Kim, E.J., Savage, T.K., Lagace, D.C., Mandyam, C.D., Eisch, A.J., Miyoshi, G., and Johnson, J.E. (2007). *Ascl1* defines sequentially generated lineage-restricted neuronal and oligodendrocyte precursor cells in the spinal cord. *Development* *134*, 285–293.
- Beatty, J.A., Sullivan, M.A., Morikawa, H., and Wilson, C.J. (2012). Complex autonomous firing patterns of striatal low-threshold spike interneurons. *J. Neurophysiol.* *108*, 771–781.
- Berninger, B., Guillemot, F., and Götz, M. (2007). Directing neurotransmitter identity of neurones derived from expanded adult neural stem cells. *Eur. J. Neurosci.* *25*, 2581–2590.
- Brandt, M.D., Jessberger, S., Steiner, B., Kronenberg, G., Reuter, K., Bick-Sander, A., von der Behrens, W., and Kempermann, G. (2003). Transient calretinin expression defines early postmitotic step of neuronal differentiation in adult hippocampal neurogenesis of mice. *Mol. Cell. Neurosci.* *24*, 603–613.
- Bylund, M., Andersson, E., Novitch, B.G., and Muhr, J. (2003). Vertebrate neurogenesis is counteracted by Sox1-3 activity. *Nat. Neurosci.* *6*, 1162–1168.
- Casarosa, S., Fode, C., and Guillemot, F. (1999). *Mash1* regulates neurogenesis in the ventral telencephalon. *Development* *126*, 525–534.
- Chanda, S., Ang, C.E., Davila, J., Pak, C., Mall, M., Lee, Q.Y., Ahlenius, H., Jung, S.W., Südhof, T.C., and Wernig, M. (2014). Generation of induced neuronal cells by the single reprogramming factor ASCL1. *Stem Cell Rev.* *3*, 282–296.
- Cherry, A.B., and Daley, G.Q. (2012). Reprogramming cellular identity for regenerative medicine. *Cell* *148*, 1110–1122.
- Doetsch, F. (2003). The glial identity of neural stem cells. *Nat. Neurosci.* *6*, 1127–1134.
- Feng, L., Hatten, M.E., and Heintz, N. (1994). Brain lipid-binding protein (BLBP): a novel signaling system in the developing mammalian CNS. *Neuron* *12*, 895–908.
- Gage, F.H. (2000). Mammalian neural stem cells. *Science* *287*, 1433–1438.
- Guo, Z., Zhang, L., Wu, Z., Chen, Y., Wang, F., and Chen, G. (2014). In vivo direct reprogramming of reactive glial cells into functional neurons after brain injury and in an Alzheimer's disease model. *Cell Stem Cell* *14*, 188–202.
- Häusser, M., Raman, I.M., Otis, T., Smith, S.L., Nelson, A., du Lac, S., Loewenstein, Y., Mahon, S., Pennartz, C., Cohen, I., and Yarom, Y. (2004). The beat goes on: spontaneous firing in mammalian neuronal microcircuits. *J. Neurosci.* *24*, 9215–9219.
- Heinrich, C., Blum, R., Gascón, S., Masserdotti, G., Tripathi, P., Sánchez, R., Tiedt, S., Schroeder, T., Götz, M., and Berninger, B. (2010). Directing astroglia from the cerebral cortex into subtype specific functional neurons. *PLoS Biol.* *8*, e1000373.
- Heinrich, C., Gascón, S., Masserdotti, G., Lepier, A., Sanchez, R., Simon-Ebert, T., Schroeder, T., Götz, M., and Berninger, B. (2011). Generation of subtype-specific neurons from postnatal astroglia of the mouse cerebral cortex. *Nat. Protoc.* *6*, 214–228.
- Heinrich, C., Götz, M., and Berninger, B. (2012). Reprogramming of postnatal astroglia of the mouse neocortex into functional, synapse-forming neurons. *Methods Mol. Biol.* *814*, 485–498.
- Heinrich, C., Bergami, M., Gascón, S., Lepier, A., Viganò, F., Dimou, L., Sutor, B., Berninger, B., and Götz, M. (2014). *Sox2*-mediated conversion of NG2 glia into induced neurons in the injured adult cerebral cortex. *Stem Cell Reports* *3*, 1000–1014.
- Hsieh, J. (2012). Orchestrating transcriptional control of adult neurogenesis. *Genes Dev.* *26*, 1010–1021.
- Jessberger, S., Toni, N., Clemenson, G.D., Jr., Ray, J., and Gage, F.H. (2008). Directed differentiation of hippocampal stem/progenitor cells in the adult brain. *Nat. Neurosci.* *11*, 888–893.
- Karimi-Abdolrezaee, S., and Billakanti, R. (2012). Reactive astrogliosis after spinal cord injury—beneficial and detrimental effects. *Mol. Neurobiol.* *46*, 251–264.



- Karow, M., Sánchez, R., Schichor, C., Masserdotti, G., Ortega, F., Heinrich, C., Gascón, S., Khan, M.A., Lie, D.C., Dellavalle, A., et al. (2012). Reprogramming of pericyte-derived cells of the adult human brain into induced neuronal cells. *Cell Stem Cell* **11**, 471–476.
- Kempermann, G., Jessberger, S., Steiner, B., and Kronenberg, G. (2004). Milestones of neuronal development in the adult hippocampus. *Trends Neurosci.* **27**, 447–452.
- Kim, E.J., Leung, C.T., Reed, R.R., and Johnson, J.E. (2007). In vivo analysis of Ascl1 defined progenitors reveals distinct developmental dynamics during adult neurogenesis and gliogenesis. *J. Neurosci.* **27**, 12764–12774.
- Kim, E.J., Battiste, J., Nakagawa, Y., and Johnson, J.E. (2008). Ascl1 (Mash1) lineage cells contribute to discrete cell populations in CNS architecture. *Mol. Cell. Neurosci.* **38**, 595–606.
- Kim, J., Efe, J.A., Zhu, S., Talantova, M., Yuan, X., Wang, S., Lipton, S.A., Zhang, K., and Ding, S. (2011a). Direct reprogramming of mouse fibroblasts to neural progenitors. *Proc. Natl. Acad. Sci. USA* **108**, 7838–7843.
- Kim, E.J., Ables, J.L., Dickel, L.K., Eisch, A.J., and Johnson, J.E. (2011b). Ascl1 (Mash1) defines cells with long-term neurogenic potential in subgranular and subventricular zones in adult mouse brain. *PLoS ONE* **6**, e18472.
- Kriegstein, A., and Alvarez-Buylla, A. (2009). The glial nature of embryonic and adult neural stem cells. *Annu. Rev. Neurosci.* **32**, 149–184.
- Kuo, C.T., Mirzadeh, Z., Soriano-Navarro, M., Rasin, M., Wang, D., Shen, J., Sestan, N., Garcia-Verdugo, J., Alvarez-Buylla, A., Jan, L.Y., and Jan, Y.N. (2006). Postnatal deletion of Numb/Numblike reveals repair and remodeling capacity in the subventricular neurogenic niche. *Cell* **127**, 1253–1264.
- Lagace, D.C., Whitman, M.C., Noonan, M.A., Ables, J.L., DeCarolis, N.A., Arguello, A.A., Donovan, M.H., Fischer, S.J., Farnbauch, L.A., Beech, R.D., et al. (2007). Dynamic contribution of nestin-expressing stem cells to adult neurogenesis. *J. Neurosci.* **27**, 12623–12629.
- Lie, D.C., Song, H., Colamarino, S.A., Ming, G.L., and Gage, F.H. (2004). Neurogenesis in the adult brain: new strategies for central nervous system diseases. *Annu. Rev. Pharmacol. Toxicol.* **44**, 399–421.
- Liu, M.L., Zang, T., Zou, Y., Chang, J.C., Gibson, J.R., Huber, K.M., and Zhang, C.L. (2013). Small molecules enable neurogenin 2 to efficiently convert human fibroblasts into cholinergic neurons. *Nat Commun* **4**, 2183.
- Lugert, S., Vogt, M., Tchorz, J.S., Müller, M., Giachino, C., and Taylor, V. (2012). Homeostatic neurogenesis in the adult hippocampus does not involve amplification of Ascl1(high) intermediate progenitors. *Nat Commun* **3**, 670.
- Ma, D.K., Bonaguidi, M.A., Ming, G.L., and Song, H. (2009). Adult neural stem cells in the mammalian central nervous system. *Cell Res.* **19**, 672–682.
- Maccaferri, G., and McBain, C.J. (1996). The hyperpolarization-activated current (I_h) and its contribution to pacemaker activity in rat CA1 hippocampal stratum oriens-alveus interneurons. *J. Physiol.* **497**, 119–130.
- Madisen, L., Zwingman, T.A., Sunkin, S.M., Oh, S.W., Zariwala, H.A., Gu, H., Ng, L.L., Palmiter, R.D., Hawrylycz, M.J., Jones, A.R., et al. (2010). A robust and high-throughput Cre reporting and characterization system for the whole mouse brain. *Nat. Neurosci.* **13**, 133–140.
- Matsui, T., Akamatsu, W., Nakamura, M., and Okano, H. (2014). Regeneration of the damaged central nervous system through reprogramming technology: basic concepts and potential application for cell replacement therapy. *Exp. Neurol.* **260**, 12–18.
- Nieto, M., Schuurmans, C., Britz, O., and Guillemot, F. (2001). Neural bHLH genes control the neuronal versus glial fate decision in cortical progenitors. *Neuron* **29**, 401–413.
- Niu, W., Zou, Y., Shen, C., and Zhang, C.-L. (2011). Activation of postnatal neural stem cells requires nuclear receptor TLX. *J. Neurosci.* **31**, 13816–13828.
- Niu, W., Zang, T., Zou, Y., Fang, S., Smith, D.K., Bachoo, R., and Zhang, C.L. (2013). In vivo reprogramming of astrocytes to neuroblasts in the adult brain. *Nat. Cell Biol.* **15**, 1164–1175.
- Ohnishi, K., Semi, K., Yamamoto, T., Shimizu, M., Tanaka, A., Mitsunaga, K., Okita, K., Osafune, K., Arioka, Y., Maeda, T., et al. (2014). Premature termination of reprogramming in vivo leads to cancer development through altered epigenetic regulation. *Cell* **156**, 663–677.
- Pacary, E., Heng, J., Azzarelli, R., Riou, P., Castro, D., Lebel-Potter, M., Parras, C., Bell, D.M., Ridley, A.J., Parsons, M., and Guillemot, F. (2011). Proneuronal transcription factors regulate different steps of cortical neuron migration through Rnd-mediated inhibition of RhoA signaling. *Neuron* **69**, 1069–1084.
- Qian, L., Huang, Y., Spencer, C.I., Foley, A., Vedantham, V., Liu, L., Conway, S.J., Fu, J.D., and Srivastava, D. (2012). In vivo reprogramming of murine cardiac fibroblasts into induced cardiomyocytes. *Nature* **485**, 593–598.
- Ramirez, J.M., Tryba, A.K., and Peña, F. (2004). Pacemaker neurons and neuronal networks: an integrative view. *Curr. Opin. Neurobiol.* **14**, 665–674.
- Reynolds, J.N., and Wickens, J.R. (2004). The corticostriatal input to giant aspiny interneurons in the rat: a candidate pathway for synchronising the response to reward-related cues. *Brain Res.* **1011**, 115–128.
- Ring, K.L., Tong, L.M., Balestra, M.E., Javier, R., Andrews-Zwilling, Y., Li, G., Walker, D., Zhang, W.R., Kreitzer, A.C., and Huang, Y. (2012). Direct reprogramming of mouse and human fibroblasts into multipotent neural stem cells with a single factor. *Cell Stem Cell* **11**, 100–109.
- Rymar, V.V., Sasseville, R., Luk, K.C., and Sadikot, A.F. (2004). Neurogenesis and stereological morphometry of calretinin-immunoreactive GABAergic interneurons of the neostriatum. *J. Comp. Neurol.* **469**, 325–339.
- Sarkar, A., and Hochedlinger, K. (2013). The sox family of transcription factors: versatile regulators of stem and progenitor cell fate. *Cell Stem Cell* **12**, 15–30.
- Sharott, A., Doig, N.M., Mallet, N., and Magill, P.J. (2012). Relationships between the firing of identified striatal interneurons and spontaneous and driven cortical activities in vivo. *J. Neurosci.* **32**, 13221–13236.



- Sofroniew, M.V. (2009). Molecular dissection of reactive astrogliosis and glial scar formation. *Trends Neurosci.* **32**, 638–647.
- Song, K., Nam, Y.J., Luo, X., Qi, X., Tan, W., Huang, G.N., Acharya, A., Smith, C.L., Tallquist, M.D., Neilson, E.G., et al. (2012). Heart repair by reprogramming non-myocytes with cardiac transcription factors. *Nature* **485**, 599–604.
- Srinivas, S., Watanabe, T., Lin, C.S., William, C.M., Tanabe, Y., Jessell, T.M., and Costantini, F. (2001). Cre reporter strains produced by targeted insertion of EYFP and ECFP into the ROSA26 locus. *BMC Dev. Biol.* **1**, 4.
- Steiner, B., Klempin, F., Wang, L., Kott, M., Kettenmann, H., and Kempermann, G. (2006). Type-2 cells as link between glial and neuronal lineage in adult hippocampal neurogenesis. *Glia* **54**, 805–814.
- Su, Z., Niu, W., Liu, M.L., Zou, Y., and Zhang, C.L. (2014a). In vivo conversion of astrocytes to neurons in the injured adult spinal cord. *Nat Commun* **5**, 3338.
- Su, Z., Zang, T., Liu, M.L., Wang, L.L., Niu, W., and Zhang, C.L. (2014b). Reprogramming the fate of human glioma cells to impede brain tumor development. *Cell Death Dis.* **5**, e1463.
- Suh, H., Consiglio, A., Ray, J., Sawai, T., D'Amour, K.A., and Gage, F.H. (2007). In vivo fate analysis reveals the multipotent and self-renewal capacities of Sox2+ neural stem cells in the adult hippocampus. *Cell Stem Cell* **1**, 515–528.
- Suvà, M.L., Rheinbay, E., Gillespie, S.M., Patel, A.P., Wakimoto, H., Rabkin, S.D., Riggi, N., Chi, A.S., Cahill, D.P., Nahed, B.V., et al. (2014). Reconstructing and reprogramming the tumor-propagating potential of glioblastoma stem-like cells. *Cell* **157**, 580–594.
- Takahashi, K., and Yamanaka, S. (2006). Induction of pluripotent stem cells from mouse embryonic and adult fibroblast cultures by defined factors. *Cell* **126**, 663–676.
- Tepper, J.M., Tecuapetla, F., Koós, T., and Ibáñez-Sandoval, O. (2010). Heterogeneity and diversity of striatal GABAergic interneurons. *Front Neuroanat* **4**, 150.
- Torii, Ma., Matsuzaki, F., Osumi, N., Kaibuchi, K., Nakamura, S., Casarosa, S., Guillemot, F., and Nakafuku, M. (1999). Transcription factors Mash-1 and Prox-1 delineate early steps in differentiation of neural stem cells in the developing central nervous system. *Development* **126**, 443–456.
- Torper, O., Pfisterer, U., Wolf, D.A., Pereira, M., Lau, S., Jakobsson, J., Björklund, A., Grechish, S., and Parmar, M. (2013). Generation of induced neurons via direct conversion *in vivo*. *Proc. Natl. Acad. Sci. USA* **110**, 7038–7043.
- Venere, M., Han, Y.G., Bell, R., Song, J.S., Alvarez-Buylla, A., and Blelloch, R. (2012). Sox1 marks an activated neural stem/progenitor cell in the hippocampus. *Development* **139**, 3938–3949.
- Vierbuchen, T., Ostermeier, A., Pang, Z.P., Kokubu, Y., Südhof, T.C., and Wernig, M. (2010). Direct conversion of fibroblasts to functional neurons by defined factors. *Nature* **463**, 1035–1041.
- Wang, T.W., Stromberg, G.P., Whitney, J.T., Brower, N.W., Klymkowsky, M.W., and Parent, J.M. (2006). Sox3 expression identifies neural progenitors in persistent neonatal and adult mouse forebrain germinative zones. *J. Comp. Neurol.* **497**, 88–100.
- Wu, Y., and Parent, A. (2000). Striatal interneurons expressing calretinin, parvalbumin or NADPH-diaphorase: a comparative study in the rat, monkey and human. *Brain Res.* **863**, 182–191.
- Zhou, Q., Brown, J., Kanarek, A., Rajagopal, J., and Melton, D.A. (2008). In vivo reprogramming of adult pancreatic exocrine cells to beta-cells. *Nature* **455**, 627–632.